


2000

On the Seasonal Mixed Layer Simulated by a Basin-Scale Ocean Model and the Mellor-Yamada Turbulence Scheme

Tal Ezer

Old Dominion University, tezer@odu.edu

Follow this and additional works at: https://digitalcommons.odu.edu/ccpo_pubs

 Part of the [Climate Commons](#), and the [Oceanography Commons](#)

Repository Citation

Ezer, Tal, "On the Seasonal Mixed Layer Simulated by a Basin-Scale Ocean Model and the Mellor-Yamada Turbulence Scheme" (2000). *CCPO Publications*. 126.
https://digitalcommons.odu.edu/ccpo_pubs/126

Original Publication Citation

Ezer, T. (2000). On the seasonal mixed layer simulated by a basin-scale ocean model and the Mellor-Yamada turbulence scheme. *Journal of Geophysical Research: Oceans*, 105(C7), 16843-16855. doi: 10.1029/2000JC900088

On the seasonal mixed layer simulated by a basin-scale ocean model and the Mellor-Yamada turbulence scheme

Tal Ezer

Program in Atmospheric and Oceanic Sciences, Princeton University, Princeton, New Jersey

Abstract. Seasonal changes and vertical mixing processes in the upper layers of the North Atlantic Ocean are simulated with a basin-scale sigma coordinate ocean model that uses the Mellor-Yamada turbulence closure scheme. The cause of insufficient surface mixing and a too shallow summertime thermocline, common problems of ocean models of this type, is investigated in detail by performing a series of sensitivity experiments with different surface forcing conditions and different turbulence parameterizations. A recent improvement in the parameterization of the dissipation term in the Mellor-Yamada turbulence scheme, which has shown a significant improvement in one-dimensional calculations, had a positive but relatively small influence on the three-dimensional calculations. The results quantify the improvement in the model upper ocean thermal structure as surface forcing becomes more realistic from one experiment to another, for example, when monthly mean winds are replaced by 6 hour variable winds. The inclusion of shortwave radiation penetration is especially important to prevent overly shallow model mixed layers during the summer and seems to affect not only the surface layer but also the thermal structure of the upper 200 m of the ocean. The difficulty of evaluating turbulent mixing processes in three-dimensional models due to errors in surface fluxes, spatial changes, and three-dimensional effects, as shown here, points to the important role still left for one-dimensional turbulence models in improving parameterizations used in three-dimensional realistic models.

1. Introduction

Ocean-atmosphere interaction processes involve momentum and heat transfer across the air-sea interface and turbulent mixing in the planetary boundary layer and in the oceanic surface mixed layer; these processes are not completely understood, and accurately simulating them is often difficult. The most notable change in the upper ocean thermal structure is the seasonal change in stratification resulting from the annual heating and cooling cycle and wind-induced mixing, yet large-scale ocean models often pay little attention to the accurate representation of the surface mixed layer. One category of mixed layer models includes Kraus-Turner-type depth-integrated bulk models [Kraus and Turner, 1967; Niiler, 1975; Garwood, 1977; Ravindran *et al.*, 1999], while another category of mixed layer models includes differential turbulence models such as that discussed here [Mellor and Yamada, 1974, 1982]; see Martin [1985] for a comparison between the two types of models. Turbulence models based on the Mellor-Yamada (M-Y) second-moment closure scheme [Mellor and Yamada, 1974, 1982] have been widely used in ocean and atmosphere models. In particular, the M-Y scheme is an integral part of the Princeton Ocean Model (POM) now used worldwide for applications such as operational coastal forecasting [Aikman *et al.* 1996], Gulf Stream studies [Ezer and Mellor, 1992] and large-scale climate simulations [Ezer and Mellor, 1997; Ezer, 1999]. In all those applications, accurate simulation of the surface mixed layer is important. However, most of the numerous studies

that have tested the M-Y scheme [Mellor and Durbin, 1975; Martin, 1985; Mellor, 1989; Galperin *et al.*, 1988; Kantha and Clayson, 1994; Klein, 1980; Richardson *et al.*, 1999] used one-dimensional models since most of the data are one-dimensional and one-dimensional models are more computationally efficient than three-dimensional models. Large-scale three-dimensional ocean models, while able to take into account processes that are missing from one-dimensional models, often use simplifications in surface forcing, such as using climatological data, that may affect their ability to simulate accurately the surface oceanic turbulent layer. Moreover, even one-dimensional M-Y models indicate a recurring deficiency in simulating the summertime mixed layers, which are often too shallow [Martin, 1985; Kantha and Clayson, 1994] because of insufficient mixing under very stable stratification conditions. To fix this problem, several studies have suggested different corrections to the original M-Y scheme; for example, Kantha and Clayson [1994] have added a Richardson number-dependent mixing at the bottom of the seasonal thermocline representing internal wave action. Guided by laboratory experiments, Mellor [2000] (hereinafter referred to as M00) has introduced a Richardson number-dependent dissipation correction for stable stratification. The latter correction will be tested here in a three-dimensional model. The goals of this study are thus to test the sensitivity of the upper ocean mixing to commonly used assumptions in large-scale ocean models and to test the recent correction to the M-Y turbulence scheme.

The paper is organized as follows. First, the Mellor-Yamada turbulence scheme and the numerical ocean model are briefly described in sections 2 and 3; then, the results of different model experiments are compared with observations in section 4; and finally, discussion and conclusions are offered in section 5.

Copyright 2000 by the American Geophysical Union.

Paper number 2000JC900088.
0148-0227/00/2000JC900088\$09.00

2. Mellor-Yamada Turbulence Model

A detailed description of the M-Y model and the assumptions that led to its development are given by numerous authors [Mellor and Durbin, 1975; Mellor and Yamada, 1974, 1982; M00], so it is only briefly reviewed here. The model has been applied to diverse problems and is widely used in numerical models of atmospheres and oceans; however, here the focus is only on the application of the M-Y scheme for simulations of the upper ocean mixing. Mellor and Yamada [1974, 1982] describe a hierarchy of model versions, labeled levels 1, 2, 3, and 4, with increasing complexities; here we use the so-called level 2 1/2 version, which is probably the most widely used in numerical models. In this version the vertical diffusivities for momentum and heat, K_M and K_H , are expressed by

$$K_M = q \ell S_M \quad (1a)$$

$$K_H = q \ell S_H, \quad (1b)$$

where $q^2/2$ is the turbulence kinetic energy, ℓ is the turbulence master length scale, and S_M and S_H are stability functions that depend on the Richardson number

$$G_H = \frac{\ell^2}{q^2} \frac{g}{\rho_o} \frac{\partial \tilde{\rho}}{\partial z} = -\frac{\ell^2 N^2}{q^2}. \quad (2)$$

The factor $\partial \tilde{\rho} / \partial z$ is the vertical density gradient minus the adiabatic lapse rate, g is the gravitation constant, ρ_o is a reference density value, and N^2 is the Brunt-Väisälä frequency. The stability functions' limit is toward infinity as G_H approaches the value 0.0288. Absent discretization error, model flows cannot exceed this value since stratification would have been destroyed by indefinitely large K_M and K_H . In the level 2 1/2 version of the model, q and ℓ are solutions of the prognostic equations:

$$\begin{aligned} \frac{Dq^2}{Dt} = & \frac{\partial}{\partial z} \left(K_q \frac{\partial q^2}{\partial z} \right) \\ & + 2K_M \left[\left(\frac{\partial U}{\partial z} \right)^2 + \left(\frac{\partial V}{\partial z} \right)^2 \right] \\ & + \frac{2g}{\rho_o} K_H \frac{\partial \tilde{\rho}}{\partial z} - 2\varepsilon + F_q \end{aligned} \quad (3a)$$

$$\begin{aligned} \frac{Dq^2 \ell}{Dt} = & \frac{\partial}{\partial z} \left(K_q \frac{\partial q^2 \ell}{\partial z} \right) \\ & + E_1 \ell \left\{ K_M \left[\left(\frac{\partial U}{\partial z} \right)^2 + \left(\frac{\partial V}{\partial z} \right)^2 \right] \ell + E_3 \frac{g}{\rho_o} K_H \frac{\partial \tilde{\rho}}{\partial z} \right\} \tilde{W} \\ & - \ell \varepsilon + F_\ell. \end{aligned} \quad (3b)$$

The terms on the right-hand side of (3a) are the vertical turbulence diffusion, the shear production, the buoyancy production, the dissipation, and the horizontal diffusion. \tilde{W} is a "wall proximity" function, K_q is the vertical turbulence diffusivity, and E_1 and E_3 are nondimensional constants [see Mellor and Yamada, 1982]. A background diffusivity of $2 \times 10^{-5} \text{ m}^2 \text{ s}^{-1}$ is added to K_M and K_H representing internal waves and other mixing processes not modeled by the M-Y scheme. Observed values of diapycnal mixing range widely from region to region, but this is a typical value for the Atlantic Ocean [Gregg, 1998].

Several modifications and corrections have been applied to the original M-Y model [see, e.g., Galperin et al., 1988; Kantha and Clayson, 1994]; here only the recent correction suggested by M00 has been tested. This latest correction is based on experiments that show that the turbulence in stratified fluid decayed as in the unstratified case until a critical Richardson number was reached, whence, rather abruptly, the decay process nearly ceased; the remaining decay then decreased as the Reynolds number increased. The above observation led to the following modification where the dissipation term in the previous M-Y model,

$$\varepsilon = \frac{q^3}{B_1 \ell}, \quad (4)$$

where $B_1 = 16.6$ is an empirical constant, is replaced by the Richardson number-dependent expression

$$\varepsilon = \frac{q^3}{B_1 \ell} \begin{cases} 1.0, & G_H \geq 0 \\ 1.0 - 0.9(G_H/G_{Hc})^{3/2}, & G_{Hc} < G_H < 0, \\ 0.1, & G_H \leq G_{Hc} \end{cases} \quad (5)$$

where G_{Hc} is a critical value of the Richardson number G_H . An empirical critical value of $G_{Hc} = -2.5$ has been suggested on the basis of comparisons between one-dimensional model results and observations at ocean stations November and Papa. The use of (5) significantly improved the simulation of surface temperatures compared with uncorrected turbulence calculations (which is identical to setting $G_{Hc} = -\infty$ in (5)); however, M00 also acknowledges a discrepancy between the empirical critical value and the laboratory experiments of Dickey and Mellor [1980]. (Further modification of the stability functions by M00 led to different best fit G_{Hc} .) In any case, since uncertainties in the critical value are yet to be resolved, we must rely on empirical determination for now, so we set the critical value in the three-dimensional model to that suggested by the one-dimensional experiments. Sensitivity experiments using different critical values ranging from -0.25 to -2.5 show only a small effect on the three-dimensional calculations. This insensitivity can be explained by the abrupt change in G_H at the bottom of the mixed layer and the insufficient vertical resolution in the three-dimensional model.

3. Numerical Model, Surface Forcing Fields, and Data

The numerical model used here is POM [Blumberg and Mellor, 1987]. The model domain, boundary conditions, and forcing have been set up to allow intercomparisons between different models, as part of the Data Assimilation and Model Evaluation Experiments in the North Atlantic Basin (DAMEE-NAB) as described in detail by Ezer and Mellor [2000]. Figure 1 shows the model grid and the bottom topography. The horizontal grid employs a curvilinear orthogonal system with a variable resolution ranging from 10-15 km in the Gulf of Mexico to 25-30 km in the eastern North Atlantic. The vertical sigma grid has 16 levels, with higher resolution in the upper mixed layer and lower resolution in the deep ocean. The deepest bottom topography in the model is set to 5500 m; at this depth, there are five layers in the upper 100 m, and proportionally higher vertical resolution is obtained in shallower regions (the shallowest depth in the model is 10 m). The vertical resolution is typical of that used in previous applications of POM to basin scale and Gulf Stream simulations

[Ezer and Mellor, 1992, 1994, 1997; Ezer, 1999]. The vertical mixing coefficients are provided by the M-Y turbulence model, described in section 2, while the horizontal mixing coefficients are calculated by a Smagorinsky-type formulation [Smagorinsky *et al.*, 1965]; see Ezer and Mellor [2000] for sensitivity experiments with different horizontal diffusivities.

Lateral open boundary conditions for temperature and salinity are provided by three 3° wide buffer zones, in the north, in the south, and in the eastern portion bordering the Gibraltar Straits, where model fields are relaxed toward observed monthly climatological fields. Inflow/outflows on the northern and southern open boundaries are imposed from the annual mean velocities derived from the whole Atlantic model of Ezer and Mellor [1997].

The experiments described here follow a spinup of 10 year simulations with monthly climatological forcing starting from initial conditions derived from the climatological temperature and salinity data of the Generalized Digital Environmental Model

(GDEM) [Teague *et al.*, 1990]. Surface wind stress during the spinup period is the monthly climatological wind stress of the Comprehensive Ocean-Atmosphere Data Set (COADS) analyzed by da Silva *et al.* [1994]; the annually averaged wind stress magnitude calculated from the monthly values is shown in Figure 2. The heat flux from the atmosphere to the ocean is divided into two components, the surface heat flux,

$$Q = Q_c + \left(\frac{\partial Q}{\partial T} \right)_c (T_c^0 - T_m^0) + (1 - C_1) Q_s, \quad (6a)$$

and the reminder, which is absorbed below the surface according to

$$Q_{\text{rad}}(z) = C_1 Q_s \exp(C_2 z). \quad (6b)$$

T^0 is the surface temperature and subscripts "m" and "c" represent fields obtained from the model and from the COADS

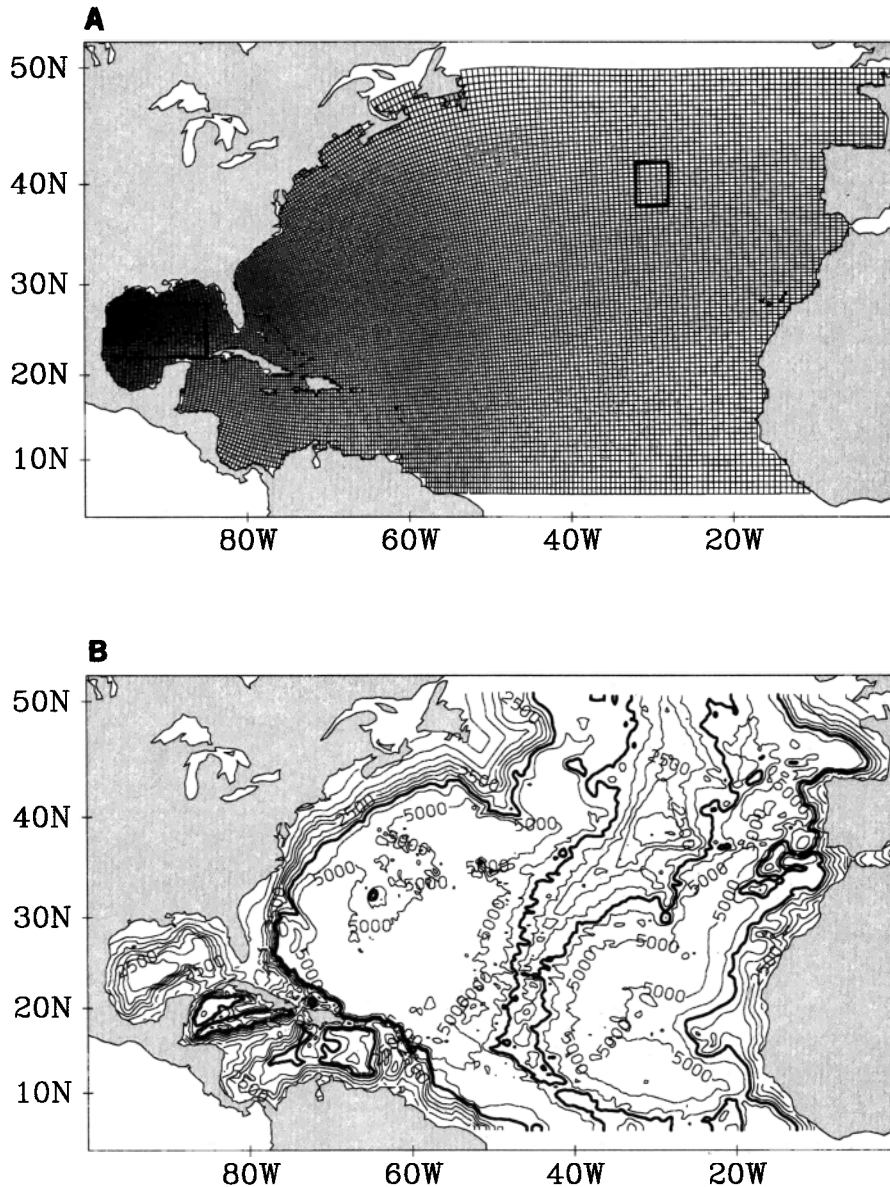


Figure 1. (a) The curvilinear model grid. The two boxed regions, one in the northeast Atlantic and one in the Gulf of Mexico, are used for detailed analysis as described in the text. (b) The model bottom topography; the contour interval is 500 m, the bold contour is 4000 m contour.

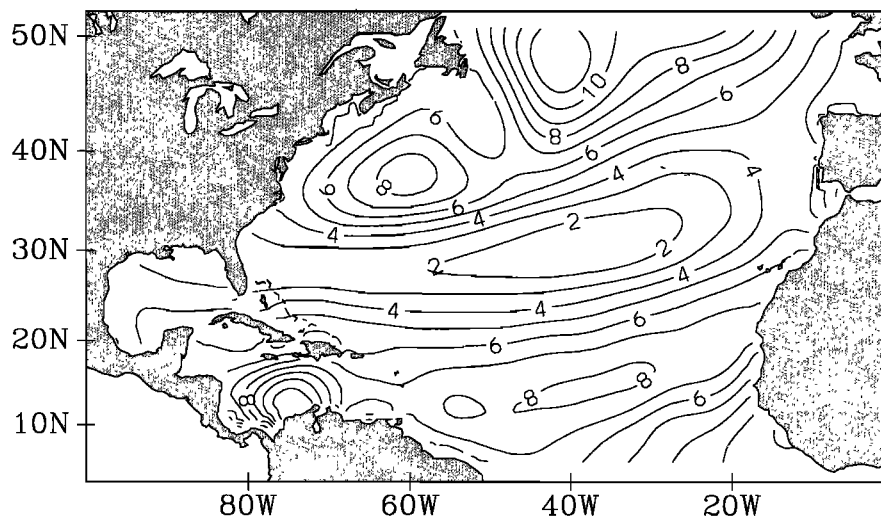


Figure 2. The annually averaged wind stress magnitude calculated from the monthly COADS climatology. The contour interval is 10^{-2} N m^{-2} .

monthly climatology, respectively. Q_s is the short wave radiation and Q_c is the total surface fluxes excluding the short wave radiation component. $C_1=0.31$ and $C_2=0.042$ are empirical attenuation coefficients corresponding to the water type IA classified by Jerlov [1976]. Martin [1985] shows that model mixed layer depth and surface temperature are quite sensitive to the choice of the water type, though here only one water type is used. The second term on the right-hand side of (6a) is a Haney-type formulation [Haney, 1971], which adds a simplified atmospheric feedback term to the observed fluxes and partly compensates for errors in the observed heat flux, assuming that the observed surface temperature is relatively more reliable than the heat flux is. The magnitude of the coupling coefficient $\partial Q/\partial T$ derived from observations is $\sim 50 \text{ W m}^{-2} \text{ K}^{-1}$, with relatively small spatial and seasonal variability. The sensitivity of the results to the coupling coefficient is explored later. The seasonal changes of the COADS heat fluxes and radiation averaged over the model domain are shown in Figure 3a. The heat fluxes applied to the surface layer of the model in run 4 (see description below) are shown in Figure 3b; they include the three terms on the right hand side of (6a). The penetrative portion of the short wave radiation (equation (6b), not shown in Figure 3b) that is absorbed below the surface is the difference between the upper curves of Figures 3a and 3b and is $\sim 30\%$ of the net incoming short wave radiation.

Salinity in the upper five layers of the model is relaxed toward the observed monthly climatology. (Experiments using surface salinity flux, where fluxes are calculated from evaporation and precipitation data, produce unrealistic results because of the lack of river runoffs and unreliable precipitation minus evaporation data.)

Four year-long experiments (runs 1-4) have been performed; they are described in the order of their degree of realism. Additional experiments to evaluate the sensitivity of the model to the choice of the coupling coefficients will be briefly described later.

1. Run 1 is similar to the spinup calculations, where surface forcing is obtained from the COADS monthly mean surface heat fluxes without short wave radiation penetration (i.e., set $C_1=0$ in (6a) and (6b)). The surface heat flux applied to the top layer of the model is thus the total heat flux in Figure 3a plus a small feedback contribution. The COADS monthly mean wind stresses are used.

2. Run 2 uses the same heat fluxes as in run 1, but wind stress anomalies in 6 hour intervals for 1993 are obtained from the European Centre for Medium-Range Weather Forecasts (ECMWF) and are added to the monthly COADS values. The 6 hour anomalies are relative to the ECMWF monthly wind stress; this procedure guarantees that large differences in the monthly values between the COADS and the ECMWF data sets are not taken into account. Figure 4 shows an example of the wind stress differences between the COADS and the ECMWF data sets. The high-frequency variations in the ECMWF winds are necessary for simulating short-term oceanic variations, but here only their effect on the seasonal thermocline will be evaluated.

3. Run 3 is similar to run 2 except that the M00 correction to the turbulence scheme, (5), is used instead of (4) for the calculations of dissipation in the model.

4. Run 4 is similar to run 3 except that short wave radiation penetration into the upper layers of the ocean is added; that is, the coefficients C_1 and C_2 in (6) are set to the values corresponding to Jerlov's water type IA, and the total surface heat flux is as in Figure 3b.

All four experiments are evaluated for a 1 year simulation starting from the same initial condition and compared with the monthly GDEM climatology. In particular, analyses of thermal structures and turbulence parameters are focused on properties averaged over two regions, the Gulf of Mexico and the northeast Atlantic; these regions are shown in Figure 1a. The model produces periodic loop current shedding of eddies, so a large averaging area is required in the Gulf of Mexico. It should be noted that using the GDEM climatology as "data" and the area-averaging procedure is useful for evaluating the three-dimensional model performance, but it does not allow direct comparisons with one-dimensional turbulence models; a direct comparison of one-dimensional models, three-dimensional models, and station data at the same point is an important, but difficult, task that was left for future studies.

4. Results

4.1. Seasonal Changes in Stratification and Mixed Layer Depth

The seasonal changes in the thermal structure of the upper 200 m obtained from the GDEM climatology are shown for the

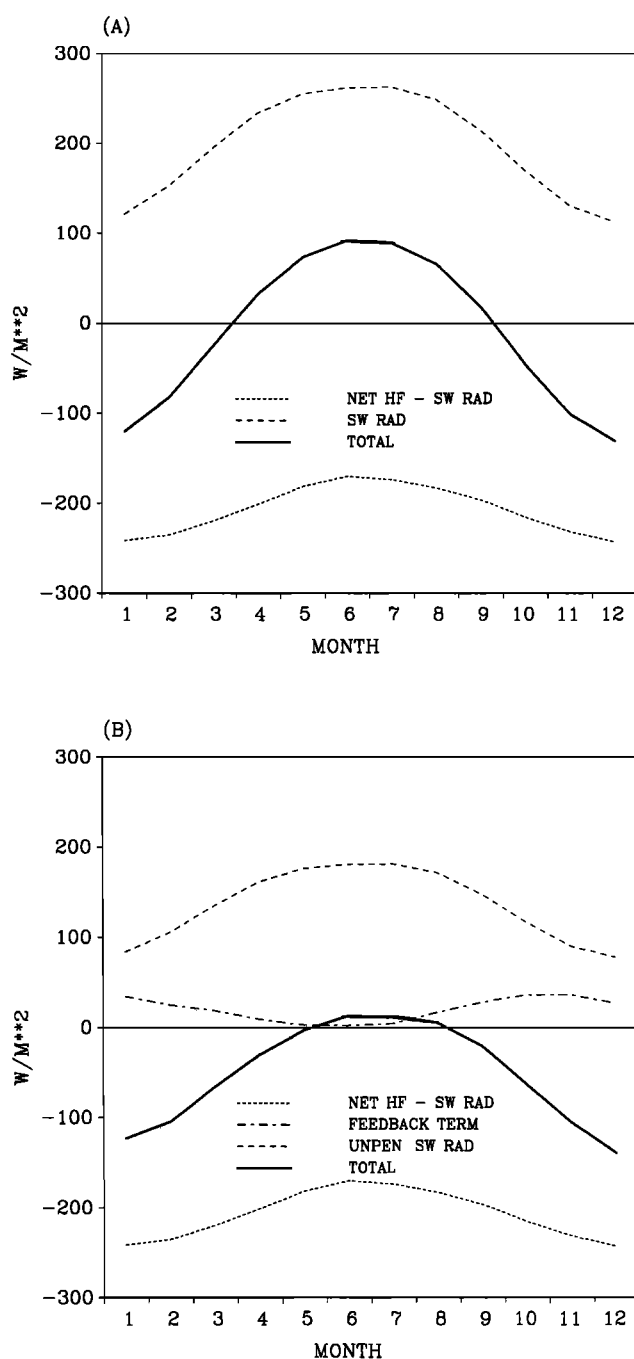


Figure 3. (a) The climatological monthly mean COADS surface fluxes averaged over the model domain. Positive values represent heating of the ocean. Incoming short wave radiation Q_s is indicated by the dashed line; the net heat flux excluding the short wave radiation Q_c is indicated by the dotted line; and the total net radiation and heat fluxes, $Q_s + Q_c$, is indicated by the heavy solid line. (b) The area-averaged monthly mean heat fluxes as applied to the surface layer of the model in run 4 (the terms on the right-hand side of (6a)). The dotted line is as in Figure 3a, the dashed line is the unpenetrated portion of Q_s that absorbs in the surface layer, the dash-dotted line is the feedback term, and the heavy solid line is the total surface heat flux.

northeast Atlantic region (Figure 5a) and for the Gulf of Mexico region (Figure 5b). In middle and high latitudes during the winter and early spring months, from December to April, the layers in the upper 200 m are well mixed; later the seasonal thermocline is built during the summer months and then deepens during the fall.

In low latitudes, only the upper 75 m are affected by the annual cycle, while the layers below 75 m remain stably stratified throughout the year (Figure 5b).

Figures 6 and 7 show the model results for the northeast Atlantic region and for the Gulf of Mexico region and should be compared with Figures 5a and 5b, respectively. The effect of different forcing and turbulence parameterization is more clear in the northeast Atlantic region (Figure 6) than in the Gulf of Mexico region (Figure 7) where the differences in the thermal structure between the different experiments is relatively small. In run 1 the summertime thermocline is clearly too shallow, and its vertical gradients are too large, but gradual improvement can be seen from one experiment to another; run 4 (Figure 6d) seems to

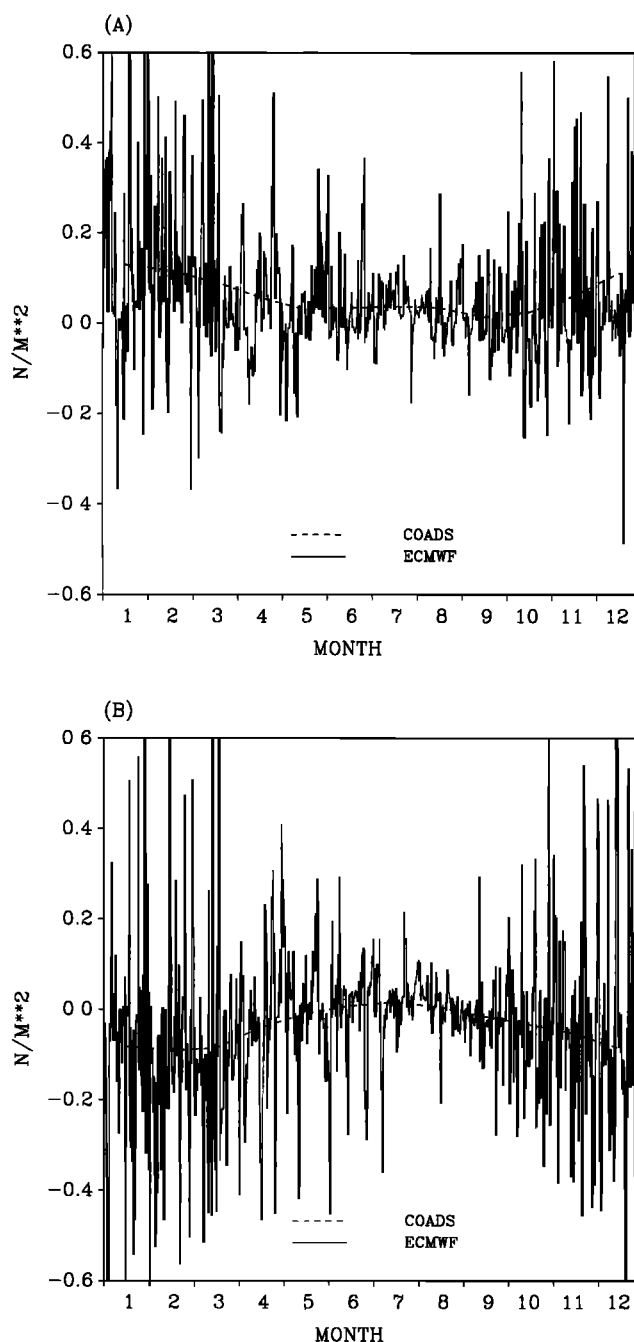


Figure 4. Wind stress components, (a) zonal and (b) meridional, at $60^\circ W$, $40^\circ N$. The COADS monthly mean wind stress is indicated by the dashed lines, and the 6 hour ECMWF wind of 1993 is indicated by the solid lines.

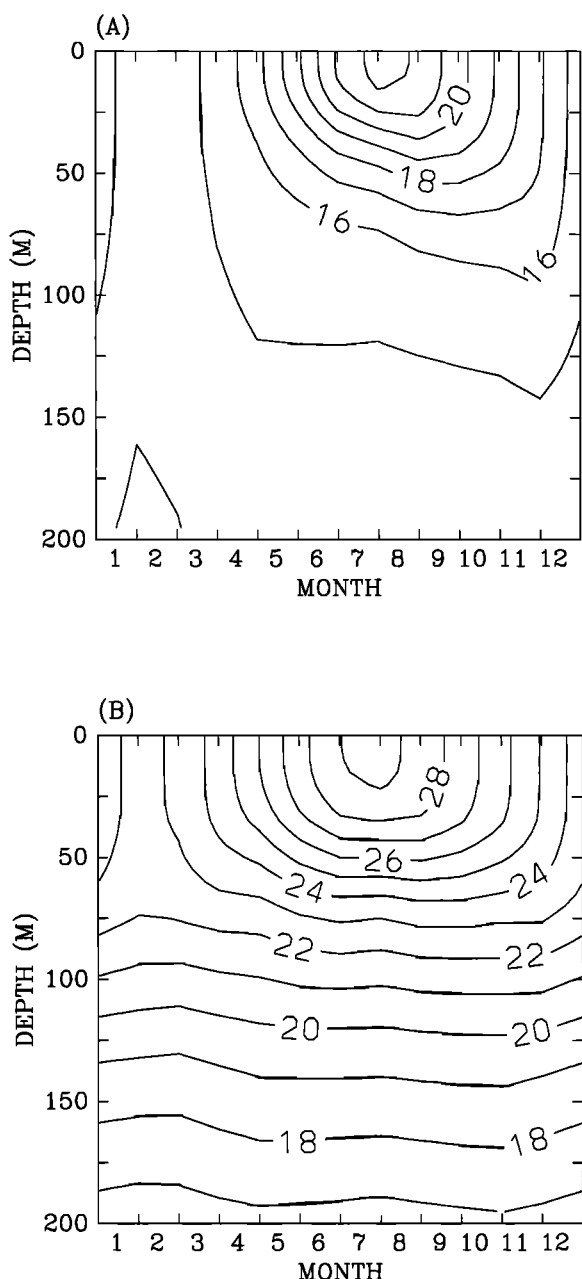


Figure 5. Area-averaged temperatures as a function of depth and time obtained from the GDEM monthly climatology for the two regions indicated in Figure 1: (a) the northeast Atlantic and (b) the Gulf of Mexico. The contour interval is 1°C.

be the most realistic one when compared with GDEM (Figure 5a). The mean surface temperature in the Gulf of Mexico exceeds 29°C from late May to mid August in run 1 (Figure 7a), while in run 4 the surface temperatures are above 29°C only from July (Figure 7d), in agreement with the observations (Figure 5b). Inclusion of the 6 hour variability in the winds in run 2 deepens the isotherms by increasing wind-steering mixing, but clearly, the wind effect, by itself, is not enough to correct the discrepancy between model and observations. The M-Y correction in run 3 further deepens the thermocline compared to run 2, and the inclusion of the short wave radiation improves the model thermal structure even further, so the discrepancy between the model calculations in run 4 and the observations is significantly decreased, though some discrepancies remain.

The spatial distribution of the depth of the mixed layer in September for the model calculations and for the GDEM climatology are shown in Figure 8. The mixed layer depth at each model grid point was found by searching for the depth where the temperature is different from the surface temperature by at least 0.5°C (for better accuracy, temperature profiles were first interpolated from the sigma grid to a high-resolution z level grid). Levitus [1982] used this definition, as well as a density-based criterion, but in the North Atlantic region the density criterion gave noisier results than the temperature criterion does. We also came to a similar conclusion analyzing the GDEM climatology. In run 1 the mixed layer depth is shallower than 10 m in the center of the subtropical gyre and between 10 and 20 m in most of the domain. The mixed layer has a maximum depth of ~40 m in the Gulf Stream region and ~30 m in the Caribbean Sea and at low latitudes (Figure 8a). In run 2 (Figure 8b) and run 3 (Figure 8c), additional wind mixing effects, especially in the eastern North Atlantic region, and the M00 correction to the turbulence scheme further deepen the mixed layer in most of the domain. However, in the three simulations the mixed layer depth is still considerably too shallow compared with the GDEM climatology (Figure 8e). The results of run 4 (Figure 8d) seem to compare best with observations relative to the other experiments, including most of the spatial variations in the mixed layer depth, though the mixed layer depth is still somewhat underestimated. Not surprisingly, the spatial distributions of the mixed layer depth in the model runs and in the observations seem to resemble the spatial distribution of the wind stress (Figure 2), which shows several regions with stronger wind forcing (and thus more intense mixing) such as in the tropical Atlantic, the Gulf Stream, and east of Newfoundland. However, note that in the Gulf Stream region all the experiments, even the ones with deficiency in the surface forcing, produce quite realistic mixed layers, indicating the insensitivity of the mixed layer to the surface forcing there.

The vertical profiles of temperatures are now compared with the GDEM climatology in the northeast Atlantic region, around 30°W and 40°N (Figure 9); the differences between the different runs are typical of those found in other regions (not shown here). A linear time interpolation between monthly GDEM values is used to obtain the observed estimates for each period. During the winter (Figure 9a), there are only negligible differences between the different experiments; all the runs have mixed layer temperatures slightly colder than the observed temperatures. In early spring (Figure 9b), model runs 1-3 show the development of shallow thermocline with no clear mixed layer, while the observations show a shallow mixed layer and a gradual cooling with depth. Run 4 shows a temperature profile closer to observations than those of the other runs. During the early summer (Figure 9c), runs 1-3 show the typical too shallow thermocline discussed before, though there is a gradual deepening of the thermocline from run 1 to run 2 (owing to additional wind mixing) and from run 2 to run 3 (owing to the M-Y dissipation correction). Run 4 seems to be the most realistic in reproducing the observed summer thermocline, though it still underestimates the thermocline depth to some extent. A similar situation prevails in late summer and early fall (Figure 9d), when surface cooling and mixing deepens the seasonal thermocline. That run 4 is significantly different than runs 1-3 is the result of the short wave radiation penetration. During the months from April to September, there is a net surface heat flux from the atmosphere to the ocean over the North Atlantic (Figure 3a) that causes warming at the surface when all the heat flux is applied as surface heating. On the other hand, when short wave radiation

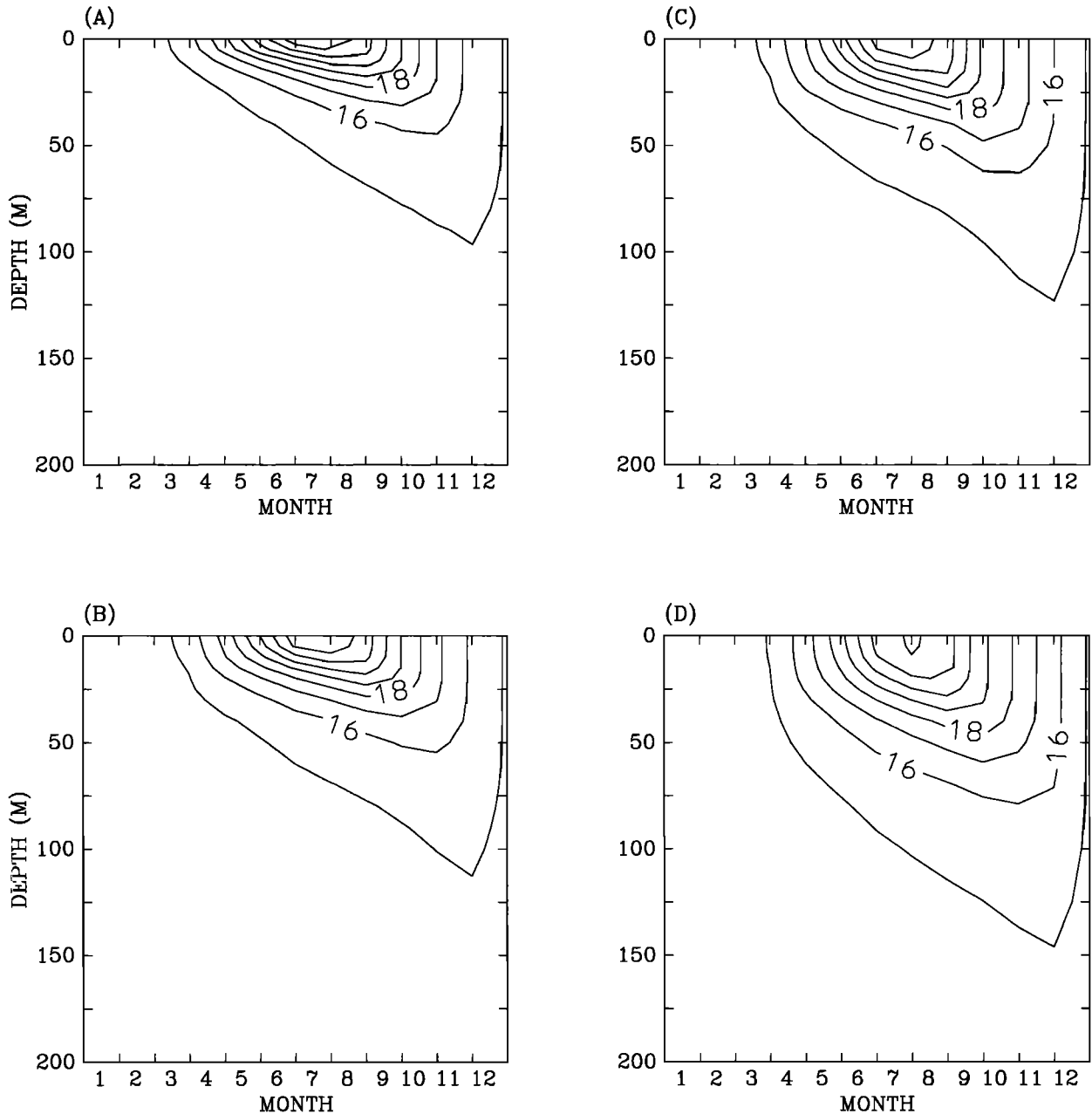


Figure 6. Area-averaged and monthly averaged temperatures as a function of depth and time for the northeast Atlantic region: (a) run 1, (b) run 2, (c) run 3, and (d) run 4. The contour interval is 1°C.

penetration is allowed in run 4, there is a net surface heat loss from the ocean surface most of the year, and the summer heating occurs mostly by the absorption of radiation below the surface (Figure 3b). The result is a reduction in the stability of the upper layer and increased mixing.

4.2. Vertical Mixing

Next, we look in more detail at the mixing processes in late summer to get a better understanding of the causes of the differences in the different runs. The vertical mixing coefficients as expressed in (1), K_M and K_H , are proportional to three turbulence properties, the turbulence velocity q , the master length scale ℓ , and the stability factors, S_M and S_H . The vertical profiles of these properties are shown in Figure 10 (note that in Figure 10c the $\log(S_M)$ is plotted for better clarity). The values are for September

30 and averaged over the northeast Atlantic region, as in Figure 9d.

The turbulence velocity (Figure 10a) indicates the increase in the values of q in the upper layers from run 1 to run 4, as expected. The difference in q between run 1 and run 2 is relatively small here because of the fact that both the COADS and ECMWF winds are quite calm during the summer and early fall months (Figure 4); during the winter months the effect of the wind variability would have been more pronounced. The effect of the M00 dissipation correction (comparing runs 1 and 2 with the old formulation to runs 3 and 4 with the new formulation) is evident in the turbulence velocity of the upper layers (Figure 10a) and in the length scales below the thermocline (Figure 10b). The modification of dissipation in (3a) and (3b) seems to cause an increase in q and ℓ and thus in turbulence mixing, especially in layers below

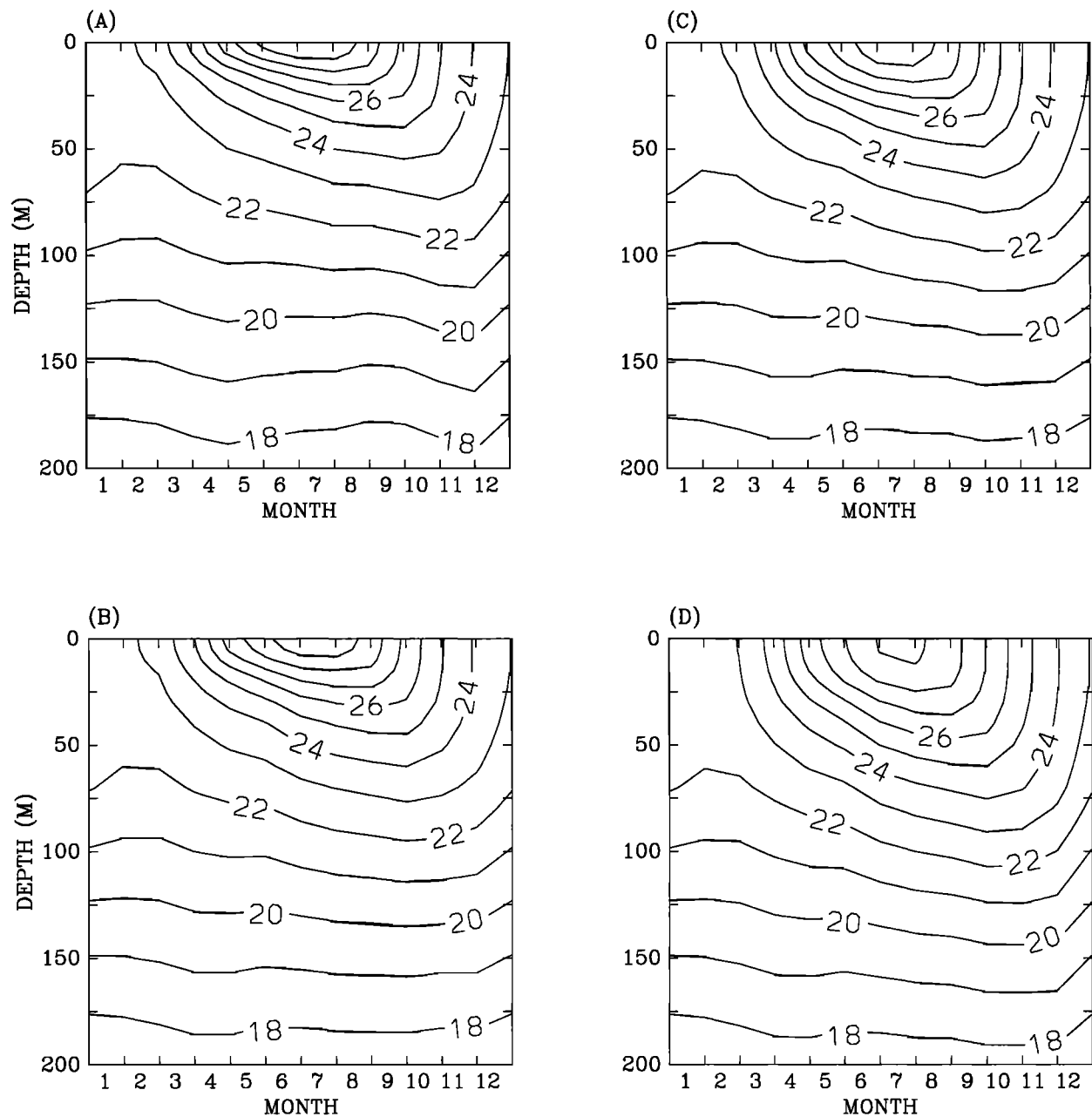


Figure 7. Same as Figure 6 but for the Gulf of Mexico region.

the thermocline, where buoyancy production and dissipation may dominate the turbulence balance.

The stability function (Figure 10c) and the diffusivity (Figure 10d) show significant and interesting differences between the different experiments. While increased instability and increased mixing in the upper layers are expected from the deepening of the mixed layer from run 1 to run 4, as discussed before, the changes in the deep layers need further explanation. An interesting and somewhat unexpected result is that a local maximum in the value of K_M is found at depths around 200 m, below the seasonal thermocline (Figure 10d); this is especially evident in run 1 and to some extent in runs 2 and 3. The turbulence velocity and the stability factor are expected to be very small below the mixed layer since shear induced mixing vanishes there and stratification should be stable as temperature drops from the warmer mixed

layer to the colder deep layers. However, this is not the case for runs 1-3, where temperature is almost well mixed just below the seasonal thermocline (Figure 9d), causing relatively large values of S_M at depth (Figure 10c). When the critical flux Richardson number, around 0.2, is reached, the turbulence is extinguished by stable stratification and $S_M \rightarrow 0$, while for unstable stratification, $S_M > 0.4$; this separation between stable and unstable layers is indicated in Figure 10c. In the deep layers below the pycnocline where wind-induced shear is small the turbulence is dominated by the buoyancy production term, and even small changes in stratification (i.e., between run 1 and run 2, Figure 9) can cause large changes in the stability factor (note the logarithmic scale in Figure 10c) and thus in the mixing coefficient. The stratification in run 1 is close enough to the threshold of unstable stability to cause an unrealistic diffusivity profile with values larger at depth

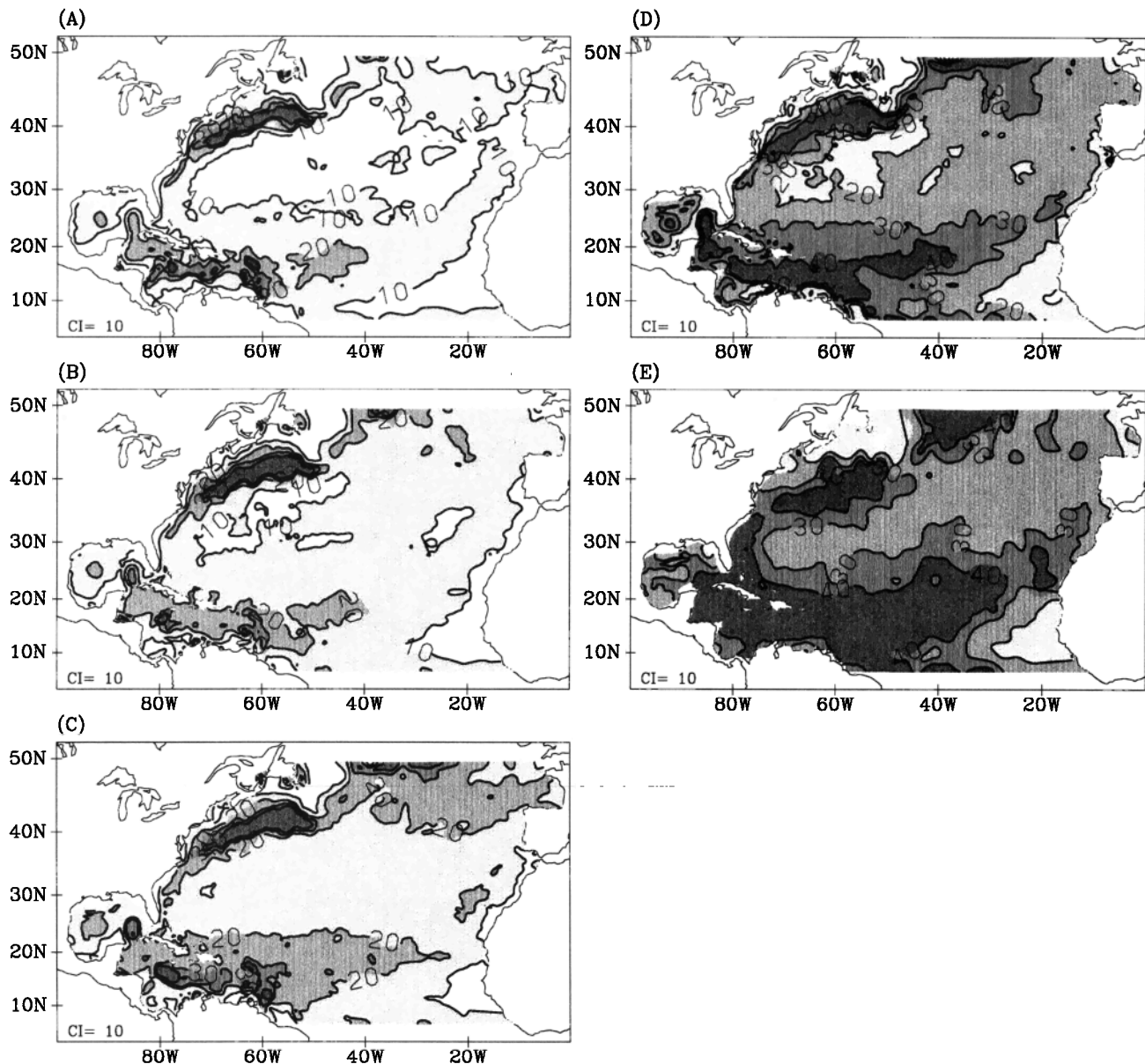


Figure 8. The depth of the mixed layer in September: (a) run 1, (b) run 2, (c) run 3, (d) run 4, and (e) GDEM climatology. The contour interval is 10 m, and darker shades represent deeper mixed layers. The bottom of the mixed layer is found from the depth where the temperature differs from the surface temperature by $>0.5^{\circ}\text{C}$.

than those in the upper layers (the large diffusivity at depth in run 1 did not cause any numerical or other problems since temperature is already well mixed there).

The reason for the significant influence of short wave radiation penetration on the stability below the seasonal thermocline is as follows: When the summertime thermocline is too shallow, the temperature gradients across the thermocline are too large and there is insufficient vertical mixing to transfer heat down from the mixed layer. As a result, the temperature at the bottom of the seasonal thermocline is too cold; for instance, at 50 m depth in September (Figure 9d) the temperature of run 1 is $\sim 3^{\circ}\text{C}$ colder than the observed temperature at that depth. Therefore the temperature at the bottom of the thermocline is almost as cold as the temperature at 200 m, creating almost a deep mixed layer at depth, with unrealistically large mixing, as discussed before.

4.3. Air-Sea Coupling Coefficient and Surface Heat Flux Errors

The temperature profiles in Figure 9 (and in other regions not shown) indicate that the heat content of the upper layers of all model runs is smaller than that observed for all seasons. This implies that in addition to uncertainties in the parameterization of turbulence in the model, the total observed surface heat flux may be underestimated. Because of the way surface heat fluxes in the model are formulated in (6), errors in the observed heat flux are compensated by the feedback term (Figure 3b). Therefore two additional experiments are performed using the same forcing and turbulence parameters as in run 4, but in one experiment the coupling coefficient $\partial Q/\partial T$ in (6) is set to zero, and in another experiment it is set to a constant value of $200 \text{ W m}^{-2} \text{ K}^{-1}$ (compared

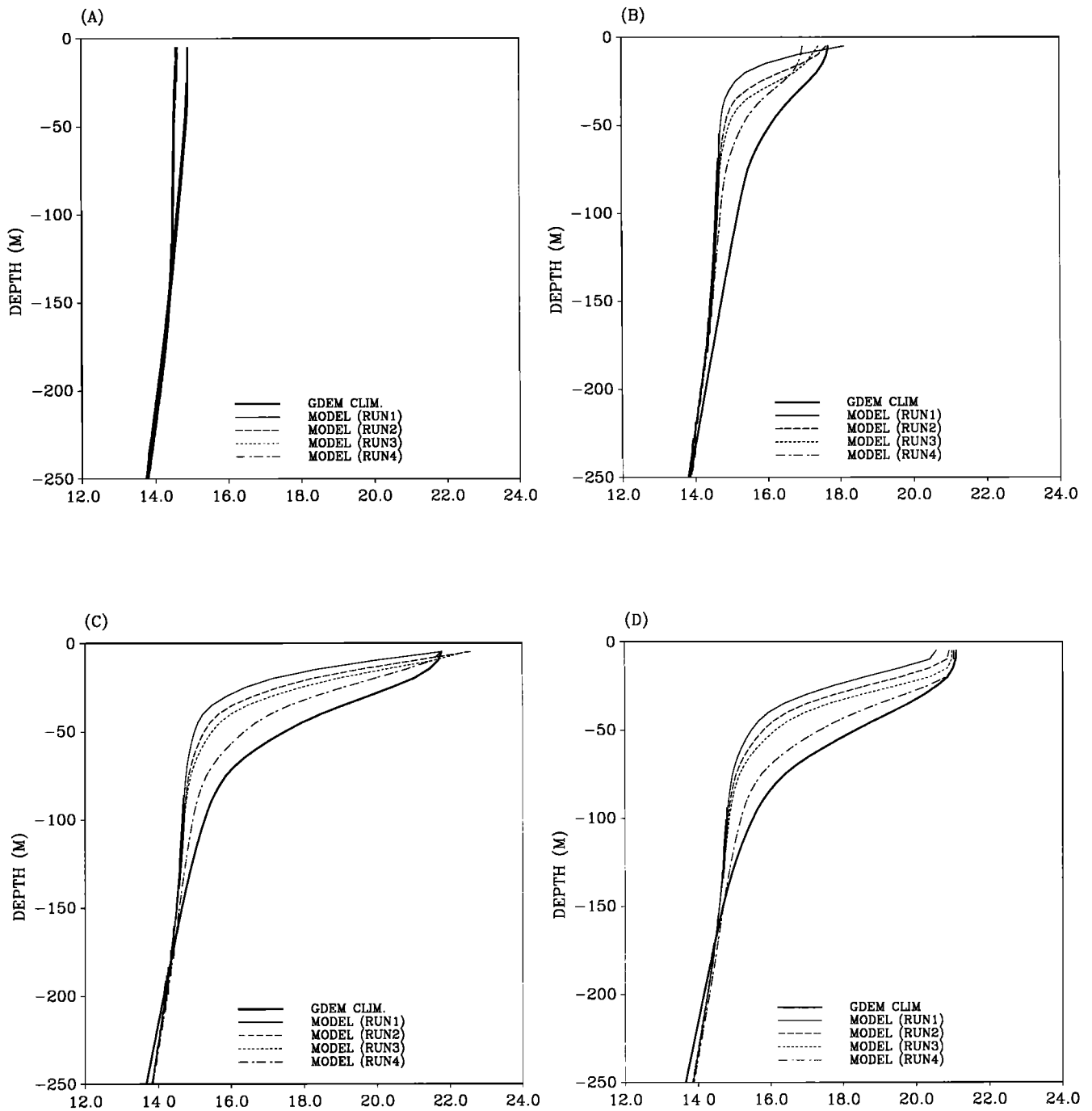


Figure 9. Vertical profiles of temperature averaged over the northeast Atlantic area indicated in Figure 1 for (a) March 30, (b) May 30, (c) July 30, and (d) September 30. Solid heavy lines are obtained from the GDEM climatology; model calculations for run 1, run 2, run 3, and run 4 are indicated by thin solid, dashed, dotted and dash-dotted lines, respectively.

to the value calculated from observations, which is $\sim 50 \text{ w m}^{-2} \text{ K}^{-1}$). A zero coupling coefficient represents a case of no air-sea feedback; thus the model heat flux is identical to the observed heat flux. A large coupling coefficient represents a case where the model heat flux is dominated by the observed surface temperature rather than by the observed surface flux (a case with $\partial Q/\partial T \rightarrow \infty$ is equivalent to forcing the model directly with the observed surface temperature, as has been done, for example, by *Ezer and Mellor [1997]*). The resultant temperature profiles of

these experiments, as well as the observed profile (same as in Figure 9d), are shown in Figure 11. In all three model calculations the depth of the mixed layer is about the same as that observed, but considerable differences in the heat content and in the surface temperature exist. Without the feedback term the surface temperature in the model at this location is smaller than the observed temperature by 1.6°C , and the heat content of the upper 200 m is only $\sim 75\%$ of the observed heat content; these results are typical for most of the model domain. The results indicate

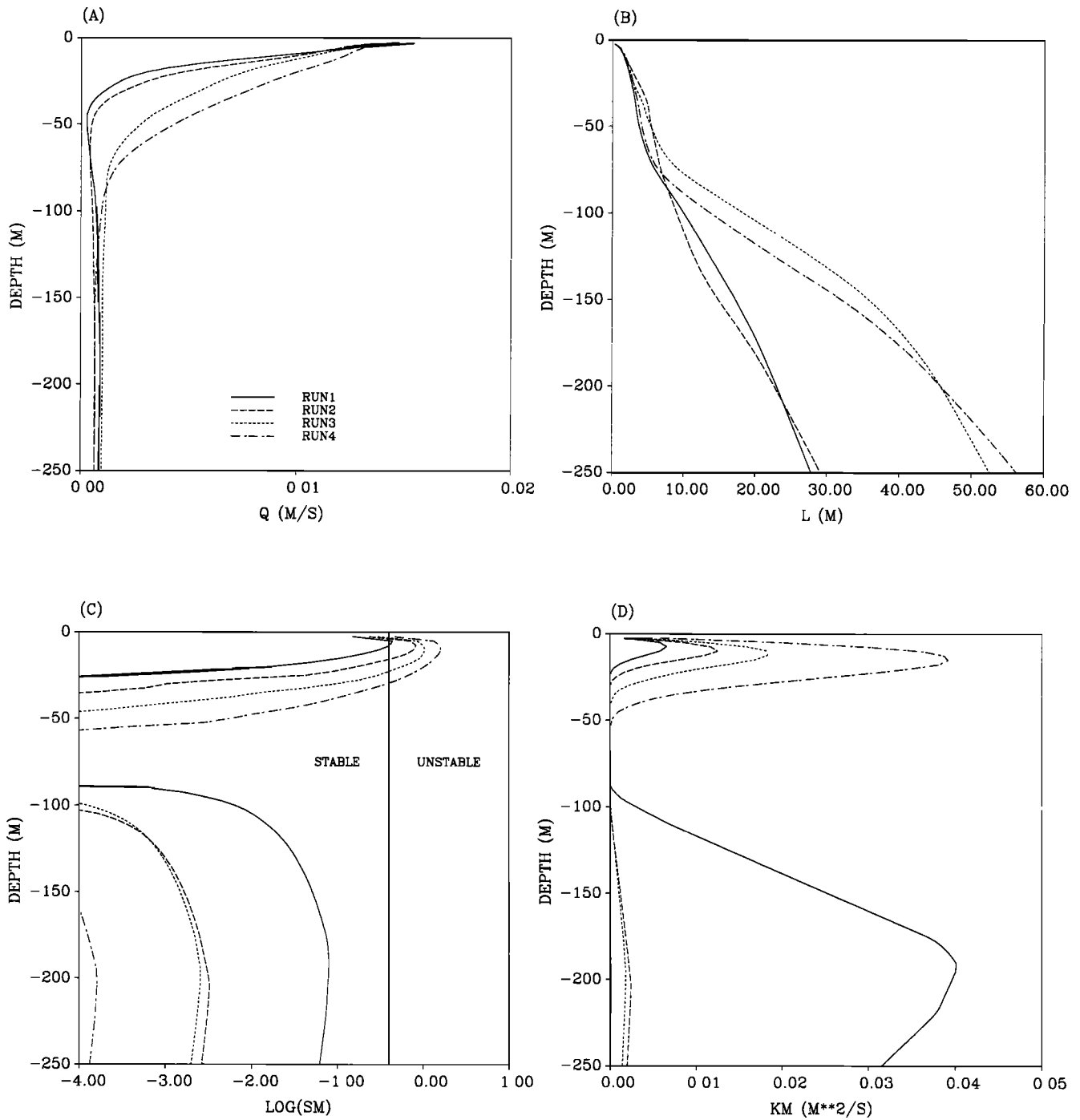


Figure 10. Vertical profiles of the turbulence parameters on September 30 averaged over the northeast Atlantic region: (a) the turbulence velocity magnitude q , (b) the turbulence length scale l , (c) log of the stability factor S_M , and (d) the vertical diffusivity coefficient K_M . Run 1, run 2, run 3, and run 4 are indicated by solid, dashed, dotted and dash-dotted lines, respectively.

that the observed COADS heat flux from the atmosphere to the ocean is underestimated and thus emphasizes the need to include a feedback term in (6) to compensate for errors in the observed fluxes. Increasing the value of the coupling coefficient to ~ 4 times the observed coefficient produces a temperature structure with heat content that is closer to the observed heat content; however, temperatures are somewhat too cold above 100 m and too warm below 100 m, where the standard case, run 4, seems to perform better. It should be noted that the feedback term, though small compared to other terms (Figure 3b), is slightly different in

each simulation, but the resultant changes in mixed layer depth and the conclusions will not be significantly affected by those differences. In fact, Figure 11 shows that even large changes in the coupling coefficient did not affect the mixed layer depth very much.

5. Discussion and Conclusions

Turbulence models based on the M-Y second-moment closure scheme [Mellor and Yamada, 1974, 1982] have been widely used

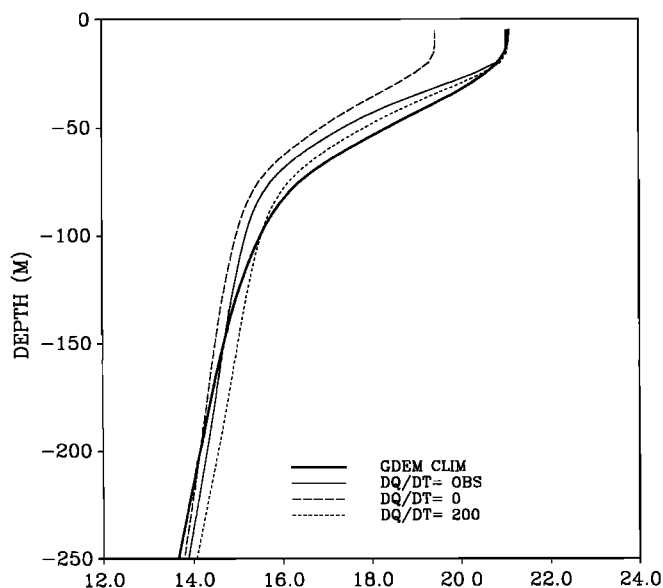


Figure 11. Vertical profiles of temperatures averaged over the northeast Atlantic area in September 30 (as in Figure 9d) for runs with different coupling coefficient $\partial Q/\partial T$. The solid, heavy line is the GDEM climatology; model calculations with $\partial Q/\partial T$ obtained from the COADS observations, i.e., spatially varied $\partial Q/\partial T$ with values around $50 \text{ W m}^{-2} \text{ K}^{-1}$ is indicated by a thin solid line, a simulation with $\partial Q/\partial T = 0$ is indicated by a dashed line and a simulation with $\partial Q/\partial T = 200 \text{ W m}^{-2} \text{ K}^{-1}$ is indicated by a dotted line.

in ocean and atmosphere models. Numerous studies, usually with one-dimensional models, evaluated its sensitivity to different parameters and forcing and compared the scheme with bulk mixed layer models and with observations [Mellor and Durbin, 1975; Martin, 1985; Mellor, 1989; Galperin et al., 1988; Kantha and Clayson, 1994; Klein, 1980; Richardson et al., 1999]. The aim of this study is to test the turbulence scheme in less idealized conditions, to test it in a three-dimensional basin-scale model, and to evaluate how assumptions that are common in surface forcing of large-scale models may affect the simulation of the oceanic surface layers. Of particular interest is the common problem of an overly shallow summertime mixed layer produced by the M-Y model [Martin, 1985; Kantha and Clayson, 1994; M00]. The chosen basin-scale model, covering the North Atlantic from 5° to 50°N including the Gulf of Mexico, has been developed for data assimilation and prediction experiments [Ezer and Mellor, 2000].

Over the model domain, there are significant spatial changes in the upper ocean mixing and thus in the depth of the seasonal thermocline and the surface mixed layer (Figure 8). While in most regions these spatial variations in the mixed layer depth seem to correspond to the spatial variations in the wind stress strength (Figure 2), as expected, in some regions like in the Gulf Stream the model mixed layer is less sensitive to changes in surface forcing since other processes such as the activity of mesoscale eddies and horizontal advection play a more important role in influencing the thermal structure and mixing of the upper ocean.

A series of experiments explore the sensitivity of the seasonal thermocline in the model to turbulence parameterization and forcing. The M-Y level 2 1/2 version, similar to the original scheme, combined with monthly climatological winds and surface heat

flux forcing produced a summertime thermocline depth that is shallower than that observed by about a factor of 2. The inclusion of higher-frequency wind variability, using 6 hour wind anomalies from the ECMWF atmospheric model, increased the upper ocean mixing, but the thermocline depth was still underestimated. Mellor [1989] and others suggest that even more frequent wind forcing is needed.

Next, the correction to the M-Y dissipation formulation of M00 has been tested; this also improves the simulations to some degree by increasing the values of the turbulence velocity and length scale (Figures 10a and 10b) calculated in (3). However, the three-dimensional model seems to be less sensitive to this correction than the one-dimensional model. For example, the simulated surface temperature at ocean station Papa changed by as much as 5°C when the dissipation correction of (5) was implemented in the one-dimensional calculations of M00. Here the feedback term in (6) does not allow such changes to occur in the three-dimensional model since it compensates for errors due to both surface heat flux and the ocean model itself. Without this feedback, results are too unrealistic (Figure 11) to perform any significant sensitivity experiments. The M00 correction introduces a critical Richardson number, G_{Hc} , which represents the critical point where dissipation starts to diminish because of stable stratification and where a transition to a regime affected by internal waves occurs. Here and in M00 the choice of the critical number is empirical. The Richardson number reached the critical number at the bottom of the mixed layer at depths following the seasonal changes of the thermocline (Figures 6 and 7). The vertical changes of G_H near the bottom of the mixed layer are very abrupt and could not be accurately calculated with the current vertical resolution. Therefore the three-dimensional model was less sensitive to the choice of G_{Hc} (as inferred from other experiments, not shown) than the one-dimensional model. In any case more research is needed to establish a way to choose the critical number.

The largest change in the model results was the inclusion of shortwave radiation penetration into the upper layers instead of the use the total net heat flux as the surface boundary condition; this result is consistent with Martin's [1985] evaluation of the sensitivity of one-dimensional simulations to shortwave radiation. The absorption of shortwave radiation below the surface, while the surface loses heat, makes the upper layers less stable, increases mixing and thus deepens the summertime thermocline. An interesting result was that small differences in parameters and forcing conditions applied to the surface model layers seemed to affect the stratification, stability and mixing coefficients of the upper few hundred meters. The overly shallow and stable thermocline in the model calculations without short wave radiation penetration is accompanied by layers below the seasonal thermocline that have too small temperature gradients, resulting in unrealistically large mixing coefficients at depths of 200–400 m. The main conclusion from these experiments is that more realistic forcing and improved parameterizations of the turbulence scheme can have a significant effect on the upper ocean thermal structure even in large-scale ocean models. One-dimensional turbulence models can still play an important role in evaluating and improving turbulence schemes used in realistic three-dimensional models. Since the heat content of the oceanic mixed layer may play an important role in climate changes, appropriate simulation of the upper ocean turbulence even in large-scale coupled ocean-atmosphere climate models may be important.

Acknowledgments. G. Mellor, B. Galperin, and anonymous reviewers provided useful comments and suggestions. The research was supported by the Office of Naval Research, Ocean Modeling Program, grants N00014-93-1-0037 and N000214-00-1-0228. Computational resources were provided by the NOAA's Geophysical Fluid Dynamics Laboratory.

References

- Aikman, F., G. L. Mellor, T. Ezer, D. Shenin, P. Chen, L. Breaker, K. Bosley, and D. B. Rao, Toward an east coast operational nowcast/forecast system, in *Modern Approaches to Data Assimilation in Ocean Modeling*, edited by P. Malanotte-Rizzoli, pp. 347-376, Elsevier Sci., New York, 1996.
- Blumberg, A. F., and G. L. Mellor, A description of a three-dimensional coastal ocean circulation model, in *Three-Dimensional Coastal Ocean Models, Coastal Estuarine Stud.*, vol. 4, edited by N. S. Heaps, 1-16, AGU, Washington, D.C., 1987.
- da Silva, A. M., C. C. Young, and S. Levitus, *Atlas of Surface Marine Data 1994*, vol. 3, *Anomalies of Heat and Momentum Fluxes*, NOAA Atlas NESDIS, vol. 8, 413 pp., Natl. Environ. Satell. Data Inf. Serv., Washington, D.C., 1994.
- Dickey, T. D., and G. L. Mellor, Decaying turbulence in neutral and stratified fluids, *J. Fluid Mech.*, 99, 13-31, 1980.
- Ezer, T., Decadal variabilities of the upper layers of the subtropical North Atlantic: An ocean model study, *J. Phys. Oceanogr.*, 29, 311-3124, 1999.
- Ezer, T., and G. L. Mellor, A numerical study of the variability and the separation of the Gulf Stream induced by surface atmospheric forcing and lateral boundary flows, *J. Phys. Oceanogr.*, 22, 660-682, 1992.
- Ezer, T., and G. L. Mellor, Diagnostic and prognostic calculations of the North Atlantic circulation and sea level using a sigma coordinate ocean model, *J. Geophys. Res.*, 99, 14,159-14,171, 1994.
- Ezer, T., and G. L. Mellor, Simulations of the Atlantic Ocean with a free surface sigma coordinate ocean model, *J. Geophys. Res.*, 102, 15,647-15,657, 1997.
- Ezer, T., and G. L. Mellor, Sensitivity studies with the North Atlantic sigma coordinate Princeton Ocean Model, *Dyn. Atmos. Oceans*, in press, 2000.
- Galperin, B., L. H. Kantha, S. Hassid, and A. Rosati, A quasi-equilibrium turbulent energy model for geophysical flows, *J. Atmos. Sci.*, 45, 55-62, 1988.
- Garwood, R. W., An oceanic mixed-layer model capable of simulating cyclic states, *J. Phys. Oceanogr.*, 7, 455-471, 1977.
- Gregg, M. C., Estimation and geography of diapycnal mixing in the stratified ocean, in *Physical Processes in Lakes and Oceans, Coastal Estuarine Stud.*, vol. 54, edited by J. Imberger, pp. 305-338, 1998.
- Haney, R., Surface thermal boundary condition for ocean circulation models, *J. Phys. Oceanogr.*, 1, 241-248, 1971.
- Jerlov, N. G., *Marine Optics*, Elsevier, New York, 231 pp., 1976.
- Kantha, L. H., and C. A. Clayson, An improved mixed layer model for geophysical applications, *J. Geophys. Res.*, 99, 25,235-25,266, 1994.
- Klein, P., A simulation of the effect of air-sea transfer variability on the structure of marine upper layers, *J. Phys. Oceanogr.*, 10, 1824-1841, 1980.
- Kraus, E. B., and J. S. Turner, A one-dimensional model of the seasonal thermocline, II, The general theory and its consequences, *Tellus*, 19, 98-105, 1967.
- Levitus, S., Climatological atlas of the world ocean, *NOAA Prof. Pap.* 13, 173 pp., U.S. Gov. Print. Off., Washington, D.C., 1982.
- Martin, P. J., Simulation of the mixed layer at OWS November and Papa with several models, *J. Geophys. Res.*, 90, 903-916, 1985.
- Mellor, G. L., Retrospect on oceanic boundary layer modeling and second moment closure, in *Parameterization of Small-Scale Processes*, edited by P. Muller and D. Henderson, pp. 251-272, Hawaii Inst. of Geophys., Honolulu, 1989.
- Mellor, G. L., One dimensional, ocean surface layer modeling, a problem and a solution, *J. Phys. Oceanogr.*, in press, 2000.
- Mellor, G. L., and P. A. Durbin, The structure and dynamics of the ocean surface mixed layer, *J. Phys. Oceanogr.*, 5, 718-728, 1975.
- Mellor, G. L., and T. Yamada, A hierarchy of turbulence closure models for planetary boundary layers, *J. Atmos. Sci.*, 13, 1791-1806, 1974.
- Mellor, G. L., and T. Yamada, Development of a turbulent closure model for geophysical fluid problems, *Rev. Geophys.*, 20, 851-875, 1982.
- Niiler, P. P., Deepening of the wind-mixed layer, *J. Mar. Res.*, 33, 405-422, 1975.
- Ravindran, P., D. G. Wright, T. Platt, and S. Sathyendranath, A generalized depth-integrated model of the oceanic mixed-layer, *J. Phys. Oceanogr.*, 29, 791-803, 1999.
- Richardson, R. A., G. G. Sutyrin, D. Hebert, and L. M. Rothstein, Universality of the modeled small-scale response of the upper tropical ocean to squall wind forcing, *J. Phys. Oceanogr.*, 29, 519-529, 1999.
- Smagorinsky, J., S. Manabe, and J. L. Holloway, Numerical results from a nine-level general circulation model of the atmosphere, *Mon. Weather Rev.*, 93, 727-768, 1965.
- Teague, W. J., M. J. Carron, and P. J. Hogan, A comparison between the Generalized Digital Environmental Model and Levitus climatologies, *J. Geophys. Res.*, 95, 7167-7183, 1990.

T. Ezer, Program in Atmospheric and Oceanic Sciences, P.O. Box CN710, Sayre Hall, Princeton University, Princeton, NJ 08544-0710. (ezer@splash.princeton.edu)

(Received July 20, 1999; revised April 7, 2000; accepted April 14, 2000.)